

Chapter 1

OPTIMAL RISK PATH ALGORITHMS*

Michael Zabaranin, Stanislav Uryasev, Panos Pardalos

Center for Applied Optimization,

Dept. of Industrial and Systems Engineering, University of Florida

zabaran@ufl.edu, uryasev@ise.ufl.edu, pardalos@ufl.edu

Abstract Analytical and discrete optimization approaches for routing an aircraft in a threat environment have been developed. Using these approaches, an aircraft's optimal risk trajectory with a constraint on the path length can be efficiently calculated. The analytical approach based on calculus of variations reduces the original risk optimization problem to the system of nonlinear differential equations. In the case of a single radar-installation, the solution of such a system is expressed by the elliptic sine. The discrete optimization approach reformulates the problem as the Weight Constrained Shortest Path Problem (WCSP) for a grid undirected graph. The WCSP is efficiently solved by the Modified Label Setting Algorithm (MLSA). Both approaches have been tested with several numerical examples. Discrete nonsmooth solutions with high precision coincide with exact continuous solutions. For the same graph, time in which the discrete optimization algorithm computes the optimal trajectory is independent of the number of radars. The discrete approach is also efficient for solving the problem using different risk functions.

Keywords: Optimal Risk Path, Length Constraint, System of Nonlinear Differential Equations, Analytical Solution, Discrete Optimization Approach, Network Flow Algorithms

Introduction

Optimal trajectory generation is a fundamental requirement for military aircraft flight management systems. These systems are required

*Research is supported by the Air Force grant F-08630-00-1-0001.

to take advantage of all available information in order to perform integrated task processing and reduce pilot workloads. The systems should provide updates at regular time intervals sufficient for threat avoidance. To optimize flight trajectory in a threat environment, a model for the risk of aircraft detection is developed based on idealizing assumptions with respect to geometrical and physical aircraft properties. An ideal flight trajectory for military operations meets the mission requirements within the constraints of aircraft limitations while minimizing risk exposure. Several levels of information are used in the selection of such a flight path and velocity profile. The trajectory can be a function of mission requirements and the threat environment. The most challenging and general problem is finding a minimal risk path, which depends on the locations of radar-installations or Surface Air Missiles (SAM), and is subject to technological constraints such as limits on flying time, fuel capacity and trajectory length.

Optimal risk path generation is closely related to optimal search path planning for calculating a route for a searcher to maximize the probability of target detecting. Basic results of the optimal search theory can be found in [16, 17, 19]. The Special Issue on Search Theory [5] contains an introductory paper by Stone and Washburn describing state-of-the-art research in this area. This issue includes a survey of the literature on the search theory containing 239 references. The most frequently used setup is to partition a search space into rectangular cells and to allocate search efforts to these cells [16, 19, 22] (see, also, various approaches with this setup in [1, 10, 20]).

In spite of numerous studies in this area, only a few considered risk optimization problems with technological constraints. The main purpose of this paper is to develop fast algorithms for optimal risk path generation with a path length constraint. These algorithms are intended for solving the optimization problem in online applications. We have considered two approaches for solving the risk optimization problem: 1) analytical solution based on calculus of variations, and 2) discrete optimization.

Using calculus of variations apparatus, we have derived the system of nonlinear differential equations for finding the optimal risk trajectory with a path length constraint in a general case. We have obtained the analytical solution of this system of differential equations in the case of a single radar-installation. The solution is expressed by the elliptic sine. Using standard mathematical software, it is illustrated with several numerical examples. Although we have made significant progress in the development of the analytical approach, construction of an analytical solution in the case with an arbitrary number of radars is still an open issue.

We have developed the discrete optimization approach for optimal path generation with a path length constraint in the case with an arbitrary number of radars. Efficiency of discrete optimization approaches for calculating optimal risk path essentially depends upon risk definition, type of technological constraints, and the aircraft's trajectory approximation (see, for instance, [21] for discussions of these issues). Many of the previous studies on trajectory generation for military aircraft are concentrated on feasible direction algorithms and dynamic programming [6]. These methods tend to be computationally intense and, therefore, are not well suited for onboard applications. To improve computation time, John and Moore [21] used simple analytical risk functions. Based on such an approach, they developed lateral and vertical algorithms to optimize flight trajectory with respect to time, fuel, aircraft final position, and risk exposure. Nevertheless, these algorithms are not intended for solving optimization problems with technological constraints, such as a constraint on the path length. In this paper, we use simple analytical functions for defining the risk and reduce optimal risk path generation with a constraint on the length to a network flow problem. An admissible domain for a flight route is approximated by a grid undirected graph and an aircraft's trajectory is presented by a path in the graph. The optimal risk path problem is reformulated as the Weight Constrained Shortest Path Problem (WCSP) for the grid undirected graph. Several network flow optimization algorithms are available for solving the WCSP [7]. For our purposes, we use the Modified Label Setting Algorithm (MLSA) with a preprocessing procedure developed and implemented in C++ code by Boland and Dumitrescu [8]. A reader interested in the WCSP and MLSA can find relevant information in [7, 8]. The original code solves problems with integer costs and weights. We have adopted and applied this code for solving risk optimization problems with real costs and weights. The efficiency of the discrete optimization approach is demonstrated with several numerical examples (various numbers of radars in different locations). Computation time in these examples is only several seconds, indicating that the MLSA is fast enough for use in online applications. However, the performance of the algorithm is evaluated only numerically. Theoretical evaluation of the algorithm's complexity is beyond the scope of this study. For the case with a single radar, we have compared analytical and numerical solutions and found that solutions coincide with high precision. This validates both analytical and discrete optimization approaches developed in this paper.

The paper is organized as follows: section 1 describes assumptions and the problem statement; section 2 presents the analytical approach; section 3 considers the discrete optimization approach; section 4 gives

concluding remarks; the Appendix contains the derivation of the system of differential equations for finding an optimal risk path with a constraint on the path length in the case with an arbitrary number of radars and the derivation of the analytical solution for this system in the case with a single radar.

1. Model description and setup of the optimization problem

This paper develops a general methodology for optimal risk path planning with a constraint on the path length. However, to be more specific, we focus primarily on risks related to radar detection. For instance, for the case with two radars, Fig. 1.1 and 1.2 illustrate an unconstrained optimal trajectory and an optimal trajectory with a length constraint, respectively. Curves in these figures correspond to level sets of the risk with the maximal values in areas close to the radars. Risk declines when an aircraft is going away from radars and increases when the aircraft approaches them. The threat models used in this study do not refer to any specific military scenario. They are simple analytical models that characterize the general nature of threats.

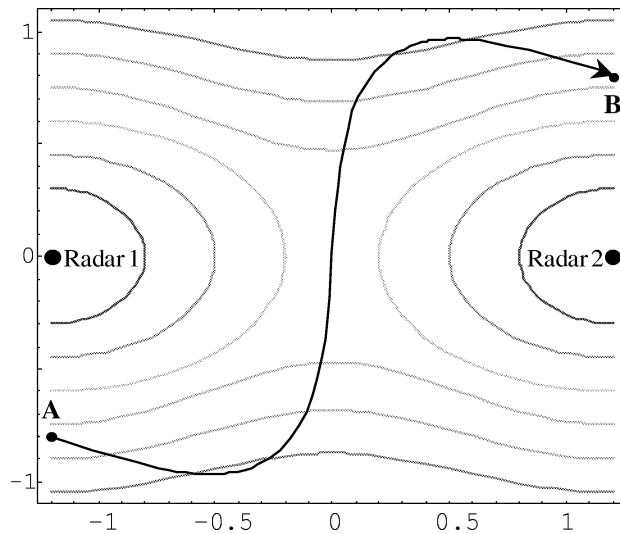


Figure 1.1. Aircraft flies from point A to point B trying to avoid two radars: optimal risk path without length constraint.

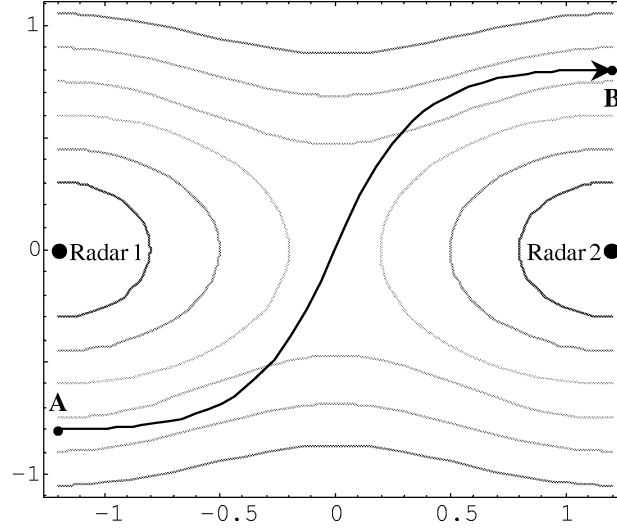


Figure 1.2. Aircraft flies from point A to point B trying to avoid two radars: optimal risk path with length constraint.

To formulate a risk path optimization problem the following assumptions are used:

1. Horizontal plane model. Aircraft position is considered to be in a horizontal plane only.
2. Radar detection of the aircraft does not depend on the aircraft's heading and climb angles.
3. Rotation angle does not depend on trajectory position.
4. An admissible domain for the aircraft's trajectory is assumed to be a detection area for all radar-installations. In other words, distance from the aircraft to each i^{th} radar-installation is not greater than the i^{th} radar maximum detection range, $R_{\max,i}$.
5. Risk is quantified in terms of the risk index per unit length for any particular aircraft location. The simplified threat model assumes that risk index r is proportional to risk factor σ and reciprocal to the squared distance from the aircraft position to the radar location (see, for instance, [21]). The risk factor, σ , depends on the radar's technical characteristics such as the maximum detection range, the minimum detectable signal, the transmitting power of the antenna, the antenna gain, and the wavelength of radar energy. It is considered that all of the radar's technical characteristics remain constant, hence, under such an assumption the risk factor, σ_i , is the constant for the i^{th} radar.

If $d_i = \sqrt{(x - a_i)^2 + (y - b_i)^2}$ is the distance from the aircraft position, (x, y) , to the i^{th} radar location, (a_i, b_i) , then the risk index, r_i , at trajectory point, (x, y) , is given by the formula $r_i(x, y) = \sigma_i d_i^{-2}$. Although, in this paper we considered that risk is reciprocal to squared distance, this assumption is not critical for the application of the developed methodology. For instance, the risk index can be expressed as $r_i(x, y) = \sigma_i d_i^{-4}$, which corresponds to the radar detection model with a signal reflected from the aircraft. In this case, the risk factor σ_i defines the aircraft radar cross section (RCS) for the i^{th} radar (see, for instance, [18]).

6. At every point of the admissible deviation domain, the cumulative risk from N radar-installations is evaluated as the sum of risks from each i^{th} radar, i. e. $r = \sum_{i=1}^N r_i = \sum_{i=1}^N \sigma_i d_i^{-2}$.

7. Aircraft velocity is assumed to be a constant, hence, time increment dt and unit length ds are linearly dependent: $ds = V_0 dt$. For convenience, we use unit length, ds , instead of time increment, dt .

8. For any particular aircraft location, (x, y) , the risk per unit length, ds , is calculated as the product of the risk index and unit length, ds , i. e. $r ds = \sum_{i=1}^N \sigma_i d_i^{-2} ds$.

9. The risk R accumulated along a path P is presented by the expression $R(P) = \int_P r ds$.

Based on model assumptions 1 – 9, the optimization problem with a constraint on the path length is formulated in the following way. Let N be the number of radars and (a_i, b_i) the location of the i^{th} radar, where $i = \overline{1, N}$. The aircraft's departure and destination points are $A(x_1, y_1)$ and $B(x_2, y_2)$, respectively. The path P from A to B is associated with the integrated risk, $R(P)$, and the total length, $l(P)$. The optimal path P_* is such a path P, which minimizes $R(P)$ subject to length constraint $l(P) \leq l_*$. The optimization problem is presented in the form

$$\begin{aligned} \min_P R(P) \\ s. t. \quad l(P) \leq l_*, \end{aligned} \tag{1}$$

where $R(P)$ and $l(P)$ are defined by the expressions

$$R(P) = \int_A^B \sum_{i=1}^N \sigma_i d_i^{-2} ds, \tag{2}$$

$$l(P) = \int_A^B ds. \quad (3)$$

To solve problem (1)-(3), analytical and discrete optimization approaches are considered.

2. Analytical solution approach for the risk path optimization problem

We use calculus of variations apparatus to obtain an analytical solution for the risk optimization problem with a constraint on the path length. This approach reduces the original problem to the system of differential equations with respect to coordinates of the optimal trajectory. The complexity of this system depends upon the type of constraints and the manner in which the trajectory is defined.

The constraint on the trajectory length given in integral form (3) leads to an isoperimetric problem of calculus of variations (general theory is given in [11, 12]). We prefer not to use integral constraints in the formulation of the problem. To reduce constraint (3) to an algebraic form, coordinates of an unknown curve are presented as functions of the current length, s , of the curve, i. e. $x = x(s)$, $y = y(s)$. Such a parameterization is also known as the natural definition of a curve. The relation between differentials of the curve arc length, ds , and curve coordinates, dx and dy , such that $ds^2 = dx^2 + dy^2$, is reduced to an additional non-holonomic constraint for derivatives of $x(s)$ and $y(s)$. In other words, if we denote $\dot{x}(s) = \frac{d}{ds}x(s)$ and $\dot{y}(s) = \frac{d}{ds}y(s)$, then $\dot{x}(s)$ and $\dot{y}(s)$ should satisfy the equality $(\dot{x}(s))^2 + (\dot{y}(s))^2 = 1$. The distance between the i^{th} radar location, (a_i, b_i) , and the aircraft position, $(x(s), y(s))$, is defined by the expression $d_i = \sqrt{(x(s) - a_i)^2 + (y(s) - b_i)^2}$. With calculus of variations, problem (1)-(3) is reduced to minimization of functional $R(l)$ with respect to unknown curve $(x(s), y(s))$, where $0 \leq s \leq l$, with boundary conditions (x_1, y_1) , (x_2, y_2) and constraint on the trajectory length, $l \leq l_*$. Problem (1)-(3) is reformulated in the form

$$\min_{(x,y)} \int_0^l \sum_{i=1}^N \sigma_i d_i^{-2} ds, \quad (4)$$

subject to boundary conditions

$$\begin{aligned} x(0) &= x_1, & x(l) &= x_2, \\ y(0) &= y_1, & y(l) &= y_2, \end{aligned} \quad (5)$$

and constraints

$$(\dot{x}(s))^2 + (\dot{y}(s))^2 = 1, \quad (6)$$

$$l \leq l_*. \quad (7)$$

Constraint $l \leq l_*$ is different from $l = l_*$, which is considered in classical calculus of variations (see, for instance, [11, 12]). In the case when $l \leq l_*$, it is a problem of calculus of variations with a moveable end point. The total variation of functional (4) must include the variation of the path length, l , and, therefore, value l is determined from an additional condition.

Let us denote the risk function in integral (4) by function L , which depends on variables x and y ,

$$L(x(s), y(s)) = \sum_{i=1}^N \sigma_i d_i^{-2}. \quad (8)$$

Calculus of variations problem (4)-(7) for finding the optimal trajectory, $(x(s), y(s))$, is reduced to the system of differential equations

$$\begin{cases} L'_x - \frac{d}{ds}(\dot{x}L) = \lambda_L \ddot{x} \\ L'_y - \frac{d}{ds}(\dot{y}L) = \lambda_L \ddot{y} \end{cases} \quad (9)$$

with boundary conditions (5) and constraint (7), where λ_L is a non-negative constant appearing due to length constraint (7). A detailed derivation of system (9) and the analytical solution for this system in the case of a single radar are included in the Appendix.

Since equation (6) is the first integral of system (9), constraint (6) and system (9) are not independent. While construction of an analytical solution of system (9) for a general form of function L is an open issue, the numerical solution for system (9) with boundary conditions (5), satisfying $l = l_*$, can be efficiently calculated by the method of weighted residuals [2, 15]. However, a numerical solution of system (9) is beyond the scope of this paper.

We have derived the analytical solution of system (9) in the case of a single radar. Without loss of generality, it is assumed that the radar is

located at the origin of the system of coordinates, i. e. $a_1 = 0$, $b_1 = 0$, and that the risk factor, σ , equals 1. To simplify calculations, the polar system of coordinates is used. The polar radius, ρ , and polar angle, Ψ , are related to Cartesian coordinates x and y in the following way

$$\begin{aligned} x(s) &= \rho(s) \cos \Psi(s), \\ y(s) &= \rho(s) \sin \Psi(s). \end{aligned}$$

Function L is rewritten as

$$L(\rho(s), \Psi(s)) = \rho^{-2}. \quad (10)$$

The optimal path has bounded length even in the case when length constraint (7) is relaxed. This is caused by the fact that function L does not converge rapidly enough to zero when ρ tends to infinity. The optimal solution for optimization problem (4)-(6) without constraint on the path length is presented by an arc of the circle

$$\left(x - (2a)^{-1} \sin C\right)^2 + \left(y - (2a)^{-1} \cos C\right)^2 = (2a)^{-2}, \quad (11)$$

where constants a and C are determined from boundary conditions (5). In the case when the constraint on the length is relaxed, the radar location, (a_1, b_1) , and the aircraft's departure and destination points, (x_1, y_1) and (x_2, y_2) , lie on the same circle. Denoting $\rho_1 = \sqrt{x_1^2 + y_1^2}$, $\rho_2 = \sqrt{x_2^2 + y_2^2}$ and the angle between vectors (x_1, y_1) , (x_2, y_2) by ϑ , such that

$$\vartheta = \arccos \left(\frac{x_1 x_2 + y_1 y_2}{\rho_1 \rho_2} \right), \quad (12)$$

the optimal risk, R_* , and unconstrained path length, \bar{l} , are expressed in terms of ρ_1 , ρ_2 and ϑ

$$R_* = \frac{1}{\rho_1 \rho_2} \sqrt{(x_2 - x_1)^2 + (y_2 - y_1)^2}, \quad (13)$$

$$\bar{l} = \frac{\vartheta}{\sin \vartheta} \sqrt{(x_2 - x_1)^2 + (y_2 - y_1)^2}. \quad (14)$$

If $\bar{l} \leq l_*$ then length constraint (7) is inactive and l coincides with \bar{l} . The optimal solution is determined by (11)-(14). In the case when $l_* \leq \bar{l}$,

constraint (7) becomes active and l coincides with l_* . Using definition of the elliptic sine (see [3])

$$\operatorname{sn}[u, \kappa] = \sin(\operatorname{am}(u, \kappa)) = \sin \phi, \quad u = \int_0^\phi \frac{dt}{\sqrt{1 - \kappa^2 \sin^2 t}},$$

the optimal solution for the case $l_* \leq \bar{l}$, i. e. $l = l_*$, is presented in the form

$$\rho(\Psi) = \frac{1+\kappa}{a} \operatorname{sn}\left[\frac{1}{1+\kappa}\Psi + C, \kappa\right],$$

or

$$\begin{aligned} x(\Psi) &= \frac{1+\kappa}{a} \operatorname{sn}\left[\frac{1}{1+\kappa}\Psi + C, \kappa\right] \cos \Psi, \\ y(\Psi) &= \frac{1+\kappa}{a} \operatorname{sn}\left[\frac{1}{1+\kappa}\Psi + C, \kappa\right] \sin \Psi, \end{aligned} \quad (15)$$

with boundary conditions

$$\begin{aligned} x^2 + y^2 &= \rho_1^2, & \Psi &= \Psi_1 = \arccos \frac{x_1}{\rho_1}, \\ x^2 + y^2 &= \rho_2^2, & \Psi &= \Psi_2 = \arccos \frac{x_2}{\rho_2}, \end{aligned} \quad (16)$$

where values ρ_1, ρ_2 are defined above and $0 \leq \Psi \leq \pi$.

According to (15), the optimal risk, R , and optimal path length, l , are given

$$R = \frac{a}{(1+\kappa)^2} \int_{\Psi_1}^{\Psi_2} \left(\kappa + \operatorname{sn}^{-2}\left[\frac{1}{1+\kappa}\Psi + C, \kappa\right] \right) d\Psi, \quad (17)$$

$$l = a^{-1} \int_{\Psi_1}^{\Psi_2} \left(1 + \kappa \operatorname{sn}^2\left[\frac{1}{1+\kappa}\Psi + C, \kappa\right] \right) d\Psi. \quad (18)$$

Constants a, κ , and C are determined from boundary conditions (16) and equality (18) under condition $l = l_*$.

First, the value of \bar{l} should be calculated; if $\bar{l} \leq l_*$, the optimal solution is given by (11)-(14), and if $l_* \leq \bar{l}$ the optimal path is determined by (15)-(18).

To illustrate the analytical solution for the case of a single radar, we consider the following numerical example. Suppose that the aircraft's departure and destination points are A and B with coordinates $(x_1, y_1) = (-0.25, 0.25)$, $(x_2, y_2) = (1.75, 0.25)$, respectively, and suppose that the

maximum value for the trajectory length is $l_* = 3.2$. The radar is located at $(0, 0)$ and the risk factor $\sigma = 1$. Values ϑ and \bar{l} computed according to (12), (14) are $\vartheta = \frac{\pi}{4} + \arctan 7$ and $\bar{l} = 5.536$. The length constraint is active, since $\bar{l} \geq l_*$. Parameters a , κ and, C can be calculated using standard software; we have used package *MATHEMATICA 4*. For this case, $\kappa = 0.7378$, $a = 0.9414$, $C = 3.1419$. In Fig. 1.3, curve 1 (circle arc) represents the optimal path without constraint on the length. The risk for the path and the path length are equal to 3.2 and 5.536, respectively. Curve 2 is the optimal path with constraint on the length, $l_* = 3.2$. The risk for this path is 3.326. We compare the optimal risks and trajectory lengths not only for these two curves, but also for the straight line between points A and B. The length of line AB (curve 3), l_{AB} , equals 2.0, while the risk accumulated along this line is equal to 8.857.

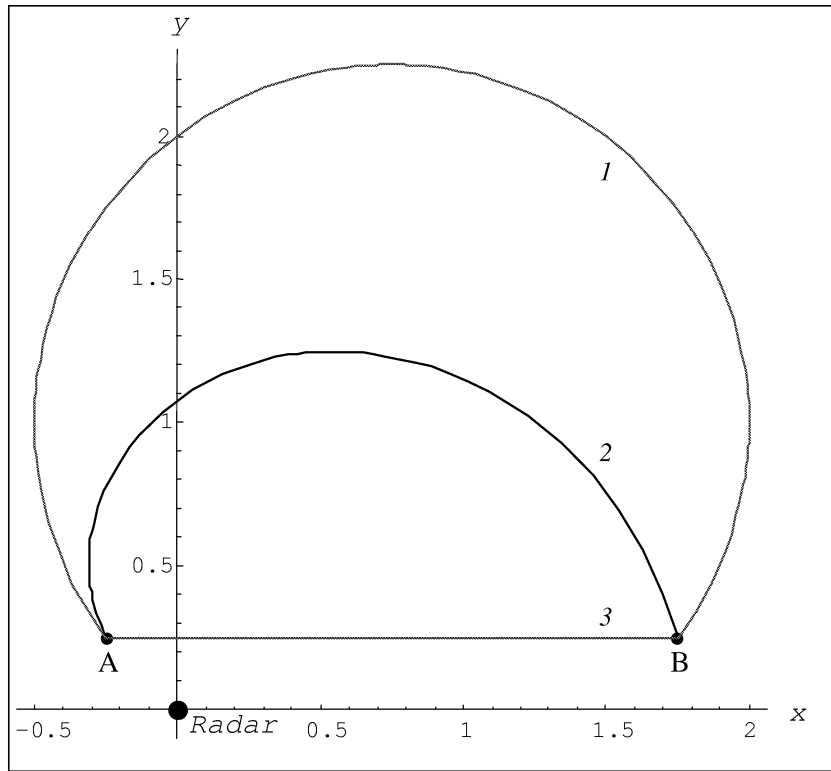


Figure 1.3. Optimal trajectories obtained by the analytical approach: curve 1 – optimal path without length constraint, $R= 3.2$, $l= 5.536$; curve 2 – optimal path with length constraint, $R= 3.326$, $l= 3.2$; curve 3 – shortest path, $R= 8.857$, $l= 2.0$

Function $R_{\min} = R(l_*)$, $l_{AB} \leq l_* \leq \bar{l}$, is concave and bounded, see Fig. 1.4.

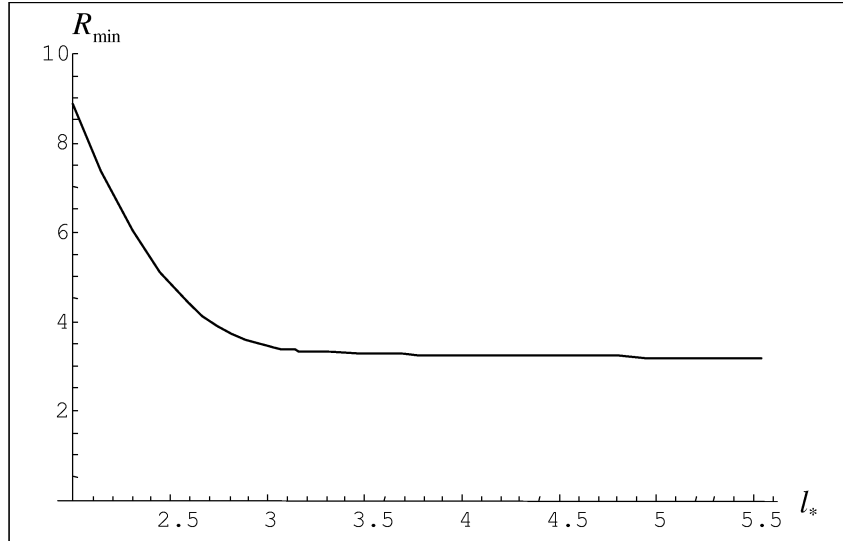


Figure 1.4. Dependence of the optimal risk on the trajectory length: the increase of the curve length greatly decreases the risk only in an area close to the radar location.

An obvious conclusion from this particular example is that the increase of the curve length considerably affects the risk only in an area close to the radar location.

3. Discrete optimization approach for optimal risk path generation with a constraint on the length

The calculus of variations approach reduces the optimization problem to solving the system of nonlinear differential equations. Construction of an analytical solution of this system for the case of an arbitrary number of radars is still an open issue. There are various numerical methods approximating a solution of the system, but that is not the focus of this paper. We propose the discrete optimization approach to directly solve the original problem. This approach reduces optimal risk path generation with a constraint on the length to the Weight Constrained Shortest Path Problem for a grid undirected graph. In the case of an arbitrary number of radars, the WCSPP can be efficiently solved by

network flow optimization algorithms. However, the computation time of these algorithms exponentially depends upon the precision prespecified for the optimal trajectory.

We assume the admissible deviation domain for the aircraft's trajectory to be an undirected graph $G = (V, A)$, where $V = \{1, \dots, n\}$ is the set consisting of n nodes and A is the set of undirected arcs. A trajectory $(x(\cdot), y(\cdot))$ is approximated by a path P in the graph G , where path P is defined as a sequence of nodes $\langle j_0, j_1, \dots, j_p \rangle$ such that $j_0 = A$, $j_p = B$ and $\langle j_{k-1}, j_k \rangle \in A$ for all k from 1 to p . To formulate (1)-(3) as a network optimization problem we use discrete approximation for formulas (2) and (3) determining the risk and trajectory length, respectively,

$$\int_A^B \left(\sum_{i=1}^N \sigma_i d_i^{-2} \right) ds = \sum_{k=1}^p \sum_{i=1}^N \sigma_i r_{i, j_{k-1} j_k} \Delta s_{j_{k-1} j_k}, \quad (19)$$

$$\int_A^B ds = \sum_{k=1}^p \Delta s_{j_{k-1} j_k}, \quad (20)$$

where $\Delta s_{j_{k-1} j_k}$ is the length of arc $\langle j_{k-1}, j_k \rangle$ and $r_{i, j_{k-1} j_k}$ denotes the risk index for the arc $\langle j_{k-1}, j_k \rangle$. If $x(j_k)$ and $y(j_k)$ are x and y coordinates for node j_k then arc length $\Delta s_{j_{k-1} j_k}$ is defined by the expression

$$\Delta s_{j_{k-1} j_k} = \sqrt{(x(j_k) - x(j_{k-1}))^2 + (y(j_k) - y(j_{k-1}))^2}. \quad (21)$$

To derive the formula for the risk index $r_{i, j_{k-1} j_k}$ we compute the risk accumulated along the arc $\langle j_{k-1}, j_k \rangle$ from the radar located at (a_i, b_i) (the risk factor σ_i is omitted for convenience)

$$\int_{j_{k-1}}^{j_k} d_i^{-2} ds = \int_{x(j_{k-1})}^{x(j_k)} \frac{\sqrt{1 + (y'_x)^2}}{(x - a_i)^2 + (y - b_i)^2} dx.$$

Since $y = y(x)$ is the straight line determined by the points $(x(j_{k-1}), y(j_{k-1}))$ and $(x(j_k), y(j_k))$, the integral above is rewritten as

$$\int_{j_{k-1}}^{j_k} d_i^{-2} ds = \frac{\left(\arctan \left(\frac{y(j_k) - b_i}{x(j_k) - a_i} \right) - \arctan \left(\frac{y(j_{k-1}) - b_i}{x(j_{k-1}) - a_i} \right) \right) \Delta s_{j_{k-1} j_k}}{(x(j_{k-1}) - a_i)(y(j_k) - b_i) - (x(j_k) - a_i)(y(j_{k-1}) - b_i)}.$$

The last formula has a simple interpretation. If we denote vector $(x(j_k) - a_i, y(j_k) - b_i)$ by \mathbf{r}_{i, j_k} , its length by $\|\mathbf{r}_{i, j_k}\|$ and the angle between two vectors $\mathbf{r}_{i, j_{k-1}}$ and \mathbf{r}_{i, j_k} by $\vartheta_{i, j_{k-1}j_k}$, where $\vartheta_{i, j_{k-1}j_k}$ satisfies condition $0 \leq \vartheta_{i, j_{k-1}j_k} \leq \pi$, then the last formula turns to the following form

$$\int_{j_{k-1}}^{j_k} d_i^{-2} ds = \frac{\vartheta_{i, j_{k-1}j_k}}{\sin \vartheta_{i, j_{k-1}j_k}} \frac{\Delta s_{j_{k-1}j_k}}{\|\mathbf{r}_{i, j_{k-1}}\| \cdot \|\mathbf{r}_{i, j_k}\|},$$

and the risk index $r_{i, j_{k-1}j_k}$ is determined as

$$r_{i, j_{k-1}j_k} = \frac{\vartheta_{i, j_{k-1}j_k}}{\sin \vartheta_{i, j_{k-1}j_k}} \|\mathbf{r}_{i, j_{k-1}}\|^{-1} \cdot \|\mathbf{r}_{i, j_k}\|^{-1}. \quad (22)$$

When $\vartheta_{i, j_{k-1}j_k}$ tends to zero, the risk index has limit value $\|\mathbf{r}_{i, j_{k-1}}\|^{-1} \cdot \|\mathbf{r}_{i, j_k}\|^{-1}$. In the limit case $\Delta s_{j_{k-1}j_k} \rightarrow 0$, i. e. $j_{k-1} \rightarrow j_k$, we have $\vartheta_{i, j_{k-1}j_k} \rightarrow 0$, $\|\mathbf{r}_{i, j_{k-1}}\| \rightarrow \|\mathbf{r}_{i, j_k}\|$ and expression (22) coincides with the risk index definition for point j_k .

Fig. 1.5 illustrates a network flow example for solving the risk minimization problem. The thick broken line is a path in the area with two radars and $\langle j_{k-1}, j_k \rangle$ is an arc of this path. The distance between nodes j_{k-1} and j_k is arc length $\Delta s_{j_{k-1}j_k}$. Values $\|\mathbf{r}_{1, j_{k-1}}\|$, $\|\mathbf{r}_{1, j_k}\|$ define distances from radar 1 to nodes j_{k-1} and j_k , respectively. Magnitude $\vartheta_{1, j_{k-1}j_k}$ corresponds to the angle between vectors $\mathbf{r}_{1, j_{k-1}}$ and \mathbf{r}_{1, j_k} .

Using substitution

$$c_{j_{k-1}j_k} = \sum_{i=1}^N \sigma_i r_{i, j_{k-1}j_k} \Delta s_{j_{k-1}j_k}, \quad (23)$$

values $R(P)$ and $l(P)$ are rearranged in the form

$$R(P) = \sum_{k=1}^p c_{j_{k-1}j_k}, \quad (24)$$

$$l(P) = \sum_{k=1}^p \Delta s_{j_{k-1}j_k}. \quad (25)$$

Thus, each arc $\langle j_{k-1}, j_k \rangle \in A$ is associated with its length $\Delta s_{j_{k-1}j_k}$ and nonnegative cost $c_{j_{k-1}j_k}$, defined by (21) and (23), respectively. Considering value $\Delta s_{j_{k-1}j_k}$ as the arc's weight we will use $R(P)$ to denote the cost of the path P and $l(P)$ to denote the total weight accumulated

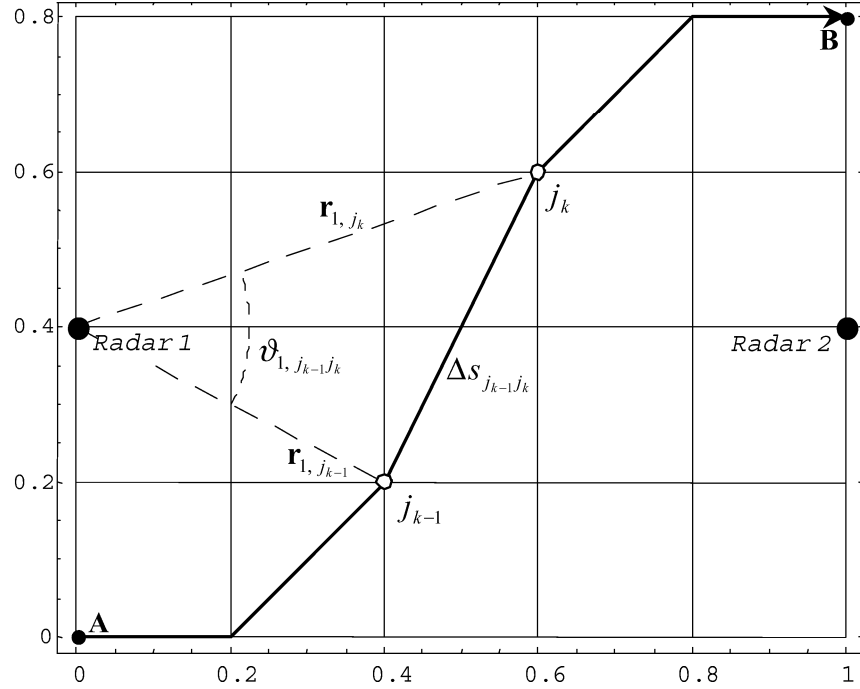


Figure 1.5. A network flow example for solving the risk minimization problem: the thick broken line AB is a path of the aircraft.

along that path. The path P is weight feasible if the total weight $l(P)$ is at most l_* , i. e. $l(P) \leq l_*$. The Weight Constrained Shortest Path Problem (WCSP) is formulated in the following way. It is required to find such a feasible path P from point A to point B that minimizes cost $R(P)$

$$\begin{aligned} \min_P \quad & \sum_{k=1}^p c_{j_{k-1} j_k} \\ \text{s. t.} \quad & \sum_{k=1}^p \Delta s_{j_{k-1} j_k} \leq l_* . \end{aligned} \quad (26)$$

The WCSP (26) is closely related to the Shortest Path Problem with Time Windows (SPPTW) and also to the Resource Constrained Shortest Path Problem (RCSPP), which uses a vector of weights, or resources, rather than a scalar. These problems are solved in column generation approaches for Vehicle Routing Problems with Time Windows (VRPTW) and in long-haul aircraft routing problems. Algorithms for solving the WCSP are divided into three major categories: label-setting algorithms based on dynamic programming methods, scaling algorithms, and algo-

gorithms based on the Lagrangean relaxation approach. The label setting algorithm is the most efficient in the case when the weights are positive [9]. The subgradient optimization [4] and cutting plane [13] methods are the core of the Lagrangean relaxation algorithm, which is efficient for solving the Lagrangean dual problem of the WCSPP in the case of one resource. Scaling algorithms use two fully polynomial approximation schemes for the WCSPP based on cost scaling and rounding [14]. The first scheme is a geometric bisection search whereas the second one iteratively extends paths. To solve the WCSPP, defined by (26), we use the Modified Label Setting Algorithm (MLSA) with a preprocessing procedure [8].

The Preprocessing Procedure and Label Setting Algorithm (LSA) are two consecutive stages of the MLSA. The LSA is the core of the MLSA, which integrates information obtained in preprocessing. The objective of the preprocessing procedure is to reduce the original graph by eliminating all arcs and nodes such that any path containing them is infeasible or does not improve current cost upper bound. To discuss the algorithm in detail, let us denote the arc's nodes j_{k-1} and j_k by i and j , respectively. For each node i , we consider the path obtained by appending the least cost path from the source node s to i to the least cost path from i to the sink node t . If the total cost accumulated along the new path is at least the current cost upper bound, then the use of node i cannot improve a known feasible solution. Hence, node i and all arcs incident to it can be deleted from the graph. If the total cost is less than the upper bound and the path is feasible, then the upper bound can be updated and the process continues with the improved upper bound. Similar, for each arc $\langle i, j \rangle$, we consider the path obtained by appending the least cost path from s to i to the least cost path from j to t , via arc $\langle i, j \rangle$. If the total cost accumulated along the new path is at least equal to the current cost upper bound, then we can delete arc $\langle i, j \rangle$ from the graph. If the total cost is less than the upper bound and the path is feasible then the upper bound can be updated. The preprocessing procedure is presented in the pseudo-code form below.

Preprocessing Algorithm for the WCSPP

Step 0: Let $U = C(n - 1)$ where $C = \max_{\langle i, j \rangle \in A} c_{ij}$.

Step 1: Find the shortest paths from source node $s = A$ with arc costs given by c_{ij} . Let Q_{sj}^c be the least cost path from s to j and α_j^c be the cost of the path: $\alpha_j^c = R(Q_{sj}^c)$.

If there is no path from s to the sink node $t = B$ **then** stop;
the problem is infeasible.

If $(l(Q_{st}^c) \leq l_*)$ **then** Q_{st}^c is the optimal path.

Step 2: Find the shortest paths from all nodes to t with arc costs given by c_{ij} . Let Q_{jt}^c be the least cost path from j to t and β_j^c be the cost of the path: $\beta_j^c = R(Q_{jt}^c)$.

Step 3: Find the shortest paths from s to all nodes with arc lengths given by Δs_{ij} . Q_{sj}^l is the shortest path from s to j and α_j^l is the length of this path: $\alpha_j^l = l(Q_{sj}^l)$.

If $(l(Q_{st}^l) > l_*)$ **then** stop; the problem is infeasible.

If $(l(Q_{st}^l) \leq l_*)$ and $(R(Q_{st}^l) < U)$ **then** set $U = R(Q_{st}^l)$.

Step 4: Find the shortest paths from all nodes to t with the arc lengths given by Δs_{ij} . Q_{jt}^l is the least length path from j to t and β_j^l is the length of this path: $\beta_j^l = l(Q_{jt}^l)$.

Step 5: **For** all $j \in V \setminus \{s, t\}$ **do**
if $(\alpha_j^l + \beta_j^l > l_*)$ **then** delete node j and all arcs incident to it;
if $(\alpha_j^c + \beta_j^c \geq U)$ **then** delete node j and all arcs incident to it;
end

Step 6: **For** all $\langle i, j \rangle \in A$ **do**
if $(\alpha_i^l + \Delta s_{ij} + \beta_j^l > l_*)$ **then** delete $\langle i, j \rangle$
else if $(\alpha_i^c + c_{ij} + \beta_j^c \geq U)$ **then** delete $\langle i, j \rangle$
else if $(l(Q_{si}^c) + \Delta s_{ij} + l(Q_{jt}^c) \leq l_*)$ **then** $U = \alpha_i^c + c_{ij} + \beta_j^c$;
end

Step 7: **If** during steps 5 and 6 the graph changed **then goto** Step 1,
else set $L = \alpha_t^c$ and stop.

End.

The next stage after the preprocessing procedure is the Label Setting Algorithm. The idea of the algorithm is to use a set of labels for each node and compare the labels to one another. Each label on a node represents a different path from node s to that node and consists of a pair of numbers representing the cost and weight of the corresponding path. No labels having the same cost are stored and for each label on a node, any other label on that node with a lower cost must have a greater weight. Let I_i be the index set of labels on node i and for each $k \in I_i$ let P_i^k denote a path from s to i with weight W_i^k and cost C_i^k . Pair (W_i^k, C_i^k) is the label of node i and P_i^k is the path corresponding to it.

For two labels (W_i^k, C_i^k) and (W_i^q, C_i^q) , corresponding to two different paths P_i^k and P_i^q , respectively, (W_i^k, C_i^k) dominates (W_i^q, C_i^q) if $W_i^k \leq W_i^q$, $C_i^k \leq C_i^q$, and the labels are not equal. Label (W_i^k, C_i^k) is efficient if it is not dominated by any other label at node i , i. e. if $(l(P), R(P))$ does not dominate (W_i^k, C_i^k) for all paths P from s to i . A path is efficient if the label it corresponds to is efficient. The LSA finds all efficient labels in every node. Starting without any labels on any node, except for label $(0, 0)$ on node s , the algorithm extends the set of all labels by treating an existing label on a node, that is, by extending the corresponding path along all outgoing arcs. Let L_i be the set of labels on node i and let $T_i \subseteq L_i$ index the labels on node i , which have been treated. The algorithm proceeds until all labels have been treated, i. e. until $L_i \setminus T_i = \emptyset$ for all $i \in V \setminus \{t\}$.

The Modified Label Setting Algorithm (MLSA)

Step 0: *Initialization*

Run Preprocessing Algorithm for the WCSP to find U , β_j^c , β_j^l and $Q_{jt}^c \quad \forall j \in V \setminus \{t\}$.
 Set $L_s = \{(0, 0)\}$ and $L_i = \emptyset$ for all $i \in V \setminus \{s\}$.
 Initialize I_i accordingly for each $i \in V$.
 Set $T_i = \emptyset$ for each $i \in V$.

Step 1: *Selection of the label to be treated*

If $\bigcup_{i \in V} (L_i \setminus T_i) = \emptyset$ **then** stop; all efficient labels have been generated.
Else choose $i \in V$ and $k \in L_i \setminus T_i$ so that W_i^k is minimal.

Step 2: *Treatment of label (W_i^k, C_i^k)*

For all $\langle i, j \rangle \in A$ **do**
If $(W_i^k + \Delta s_{ij} + \beta_j^l \leq l_*)$
If $(C_i^k + c_{ij} + \beta_j^c < U)$
If $(W_i^k + \Delta s_{ij}, C_i^k + c_{ij})$ is not dominated
 by $(W_j^q, C_j^q) \quad \forall q \in L_j$
then set $L_j = L_j \cup \{(W_i^k + \Delta s_{ij}, C_i^k + c_{ij})\}$
 and update I_j
If $(W_i^k + \Delta s_{ij} + l(Q_{jt}^c) \leq l_*)$ **then** $U = C_i^k + c_{ij} + \beta_j^c$.
end

Step 3: Set $T_i = T_i \cup \{k\}$, **goto** to Step 1.

End.

The MLSA was implemented in C++ code by Boland and Dumitrescu [8]. The code was originally designed for solving the WCSPP with integer costs and integer weights. Under the assumption of cost and weight integrality, it was shown that the WCSPP is a NP-hard problem. In the case of real costs and weights, no specific evaluation for the complexity of the MLSA is provided. It is considered that in a worse case, the WCSPP can be solved in the time exponentially depending on the number of arcs. The analysis of the MLSA's complexity is beyond the scope of this paper. The original code is adopted for solving the WCSPP with real costs and real weights assigned by (22) and (23), respectively.

For numerical examples, we use an undirected graph with nodes located in the cross-points of a square grid with the side length of T relative units. A set of arcs assigned for each node in the graph is shown in Fig. 1.6. This set consists of 32 arcs. Each arc is counted twice, since the graph is undirected. In Fig. 1.6, "1" represents four horizontal and four vertical arcs with the same length of Δs , "2" denotes eight diagonal arcs with the same length of $\sqrt{2} \Delta s$, and "3" denotes sixteen long diagonal arcs with the same length of $\sqrt{5} \Delta s$. If m is the number of arcs on the grid side, i. e. $m = T/\Delta s$, then $(m + 1)^2$ is the number of nodes and $4m(4m - 1)$ is the number of arcs in the graph.

To compare the analytical and discrete optimization approaches, we consider the previous example with a single radar. The radar location, the boundary value for the length constraint and the departure and destination points for the aircraft are exactly the same. The graph has the following characteristics: $T = 2.1$, $\Delta s = 0.05$, $m = 42$. There are 1849 nodes and 28056 arcs in this graph. All calculations have been performed using a PC 800 MHz with RAM of 256 Mb. The computation time is approximately 6 sec. Fig. 1.7 compares the analytical and discrete optimization solutions. The smooth curve is the optimal trajectory obtained by the analytical approach. The value of the risk accumulated along this trajectory equals 3.326. The nonsmooth curve is the optimal trajectory obtained by the discrete optimization approach. In this case, the trajectory has length 3.196 and risk value 3.360. For the discrete optimization solution, the relative error of the optimal risk value is about 1%. This validates both approaches.

To estimate time required for calculating the optimal trajectory with higher precision, we again consider the case with a single radar using grid undirected graph with parameters: $T = 2.1$, $\Delta s = 0.025$, and $m = 84$. There are 7225 nodes and 112560 arcs in this graph. The solution time is about 200 sec. Fig. 1.8 compares the analytical solution and discrete optimization solutions with different precision (the discrete optimiza-

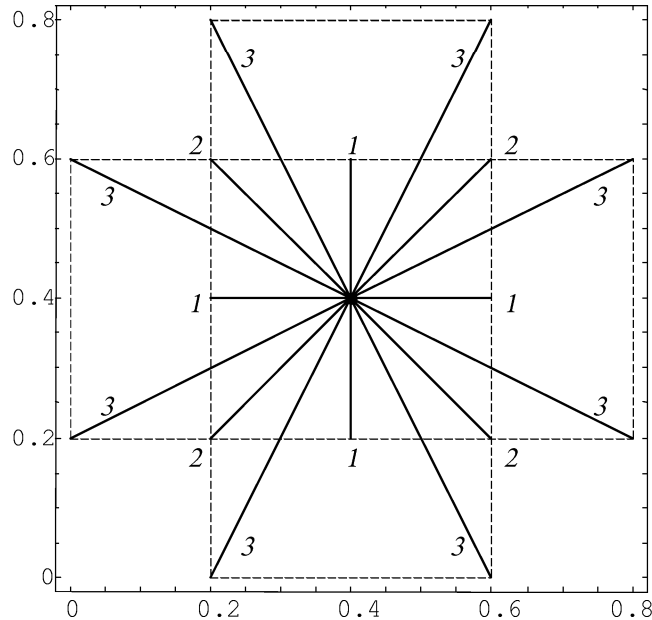


Figure 1.6. A set of arcs assigned for each node in the graph: 1 – horizontal and vertical arcs, 2 – diagonal arcs, 3 – long diagonal arcs.

tion solution with higher precision is depicted by a dashed curve). The dashed trajectory has length 3.199 and accumulated risk 3.357. The relative risk error for the dashed curve in comparison with the risk value for the analytical solution is about 0.9%. This indicates that the higher precision solution does not essentially improve the lower precision solution and that practically both trajectories are identical. In this case, the calculation time for the higher precision solution was about thirty times greater than for the lower precision solution. However, risk was improved by only 0.1%. This conclusion relates only to the considered example. In a general case, such an inference should be made based on the evaluation of the MLSA's complexity.

Computation time of the MLSA does not depend on the number of radars; it depends only on the number of arcs. To demonstrate this advantage of the discrete optimization approach, we use the same graph for calculating the optimal risk trajectories with a different number of radars. In Fig. 1.9-1.12, the optimal risk trajectories are computed in the same time interval. In all considered examples, grid undirected graph with parameters $T = 2.0$, $\Delta s = 0.02$, $m = 100$ is used, and the risk factors σ_i are assumed to be equal to 1.

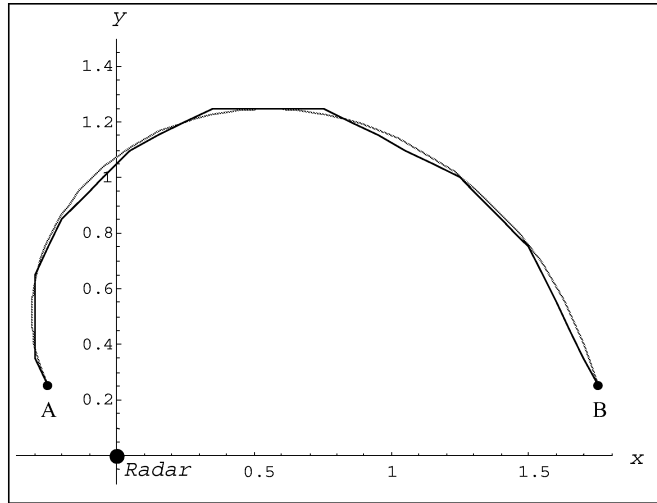


Figure 1.7. Comparison of the analytical and discrete optimization solutions: the smooth curve is the optimal path obtained by the analytical approach, $R= 3.326$, $l= 3.2$; the nonsmooth curve is the optimal path obtained by the discrete optimization approach, $R= 3.360$, $l= 3.196$

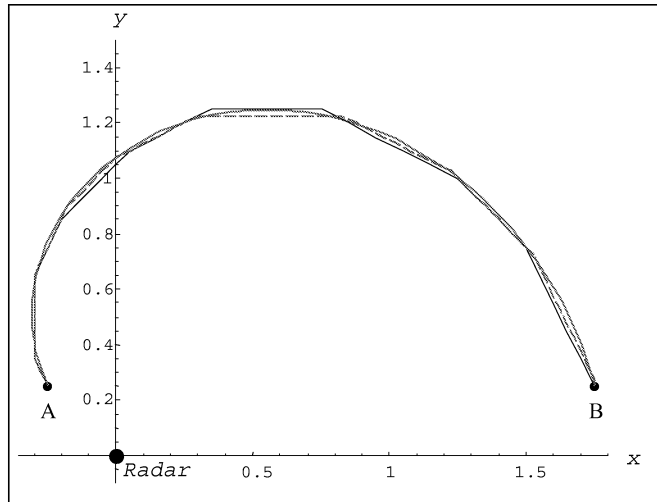


Figure 1.8. Comparison of the discrete optimization solutions with different precision: the dashed curve is the optimal discrete solution with higher precision, $R= 3.357$, $l= 3.199$; the solid nonsmooth curve is the optimal discrete solution with lower precision, $R= 3.360$, $l= 3.196$; the smooth curve is the analytical solution, $R= 3.326$, $l= 3.2$

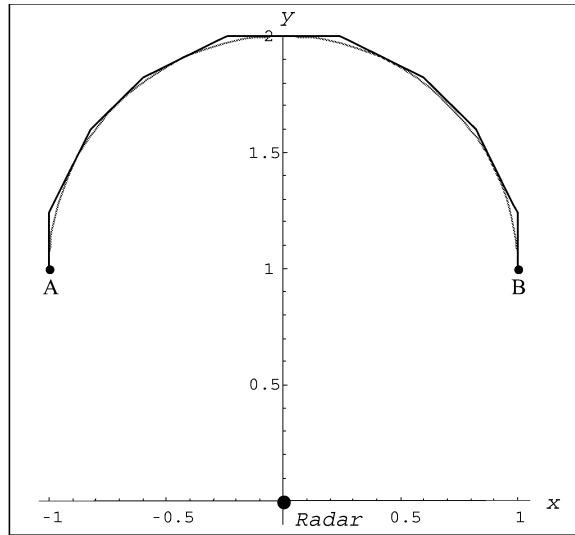


Figure 1.9. Optimal path in the case with a single radar; $T = 2.0$, $\Delta s = 0.02$, $m = 100$. The nonsmooth curve is the optimal discrete solution; the smooth curve is the analytical solution obtained by the calculus of variations approach.

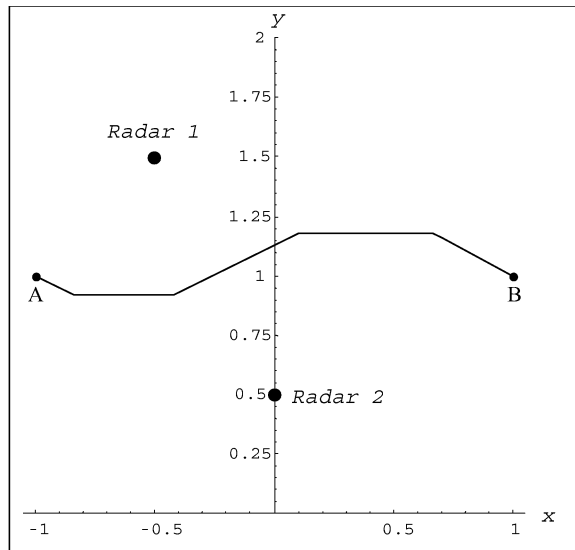


Figure 1.10. Optimal path obtained by discrete optimization in the case with two radars; $T = 2.0$, $\Delta s = 0.02$, $m = 100$.

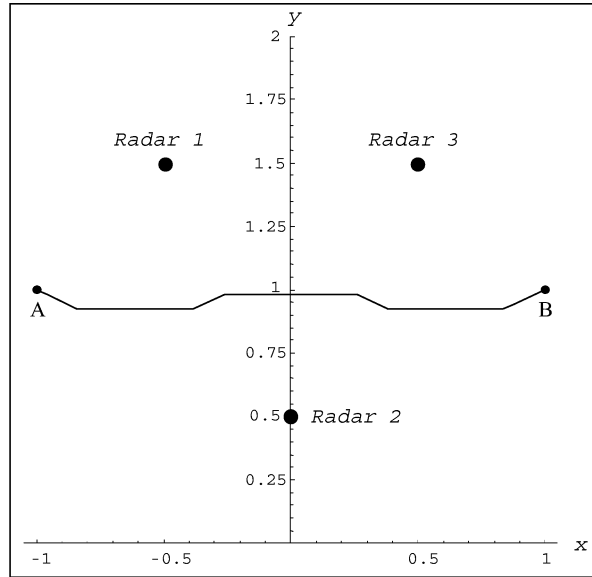


Figure 1.11. Optimal path, symmetric location of three radars; $T = 2.0$, $\Delta s = 0.02$, $m = 100$.

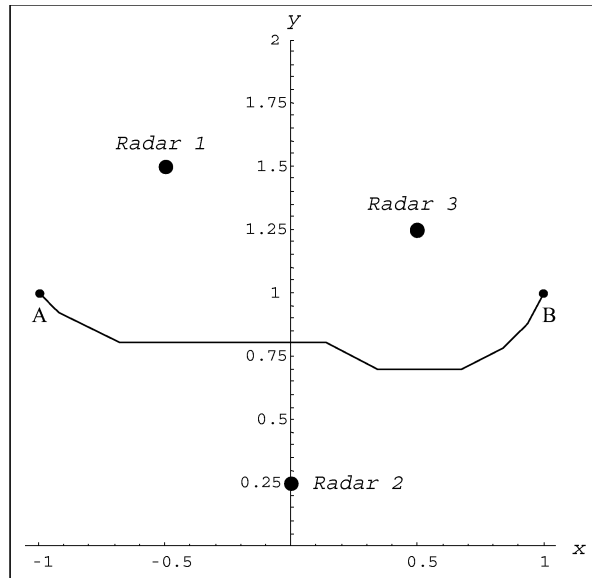


Figure 1.12. Optimal path, asymmetric location of three radars; $T = 2.0$, $\Delta s = 0.02$, $m = 100$.

4. Concluding remarks

We have developed analytical and discrete optimization approaches for calculating an optimal risk path with a constraint on the path length. We have studied optimization problems with the risk index in the form σd^{-2} (σ is the risk factor, d is the distance to the radar). However, the developed methodology is quite general and it can be used to generate optimal trajectories with other risk functions, for instance, with the risk function defined as σd^{-4} .

The analytical approach, based on calculus of variations, reduces the original problem to solving the system of nonlinear ordinary differential equations. We have derived this system using a general form of the risk function for the case with an arbitrary number of radars. For the case of a single radar and the risk function in the form σd^{-2} , we have obtained the analytical solution of the system expressed by the elliptic sine. Using the analytical solution, it is shown that the increase of the trajectory length greatly affects the risk only within an area close to the radar. Although an analytical solution for the system of differential equations can be obtained for the case with one radar and the risk function in the form σd^{-4} , an analytical solution of this system in the case with an arbitrary number of radars is still an open issue.

The discrete optimization approach reformulates the original problem as a network flow optimization problem. Using approximation for the admissible domain by a grid undirected graph and representation of a trajectory by a path in this graph, optimal risk path generation with a constraint on the length is reduced to the Weight Constrained Shortest Path Problem (WCSPP). The WCSPP is efficiently solved by the Modified Labeling Setting Algorithm (MLSA). The optimization problem with about 30000 arcs requires approximately 6 *sec* to be solved. This time is suitable for online applications. However, the precision for the MLSA should be reasonably specified, since the computation time exponentially depends on the number of arcs in the graph. We have considered several examples with a different number of radars to investigate the performance of the algorithm. The main advantages of the discrete optimization approach are: 1) it can account for an arbitrary number of radars; 2) the computation time does not depend upon the number of radars; 3) the approach can be easily implemented for various risk functions.

We have compared the analytical and discrete optimization solutions for the case with a single radar. These solutions coincide with high precision that verifies both approaches.

Acknowledgments

We want to thank Capt. R. Pendleton, USAF for helping with the development of the model for aircraft detection in a threat environment. We are also grateful to Prof. N. Boland and I. Dumitrescu for the informative discussions and for providing C++ code for the Modified Labeling Setting Algorithm that was used for conducting numerical experiments.

References

- [1] Assaf, D. and Sharlin-Bilitzky, A. (1994). *Dynamic Search for a Moving Target*. Journal for Applied Probability, Vol. 31, No. 2, pp. 438 – 457.
- [2] Aziz, A. K. (1975). *Numerical Solution of Boundary Value Problems for Ordinary Differential Equations*. New York: Academic Press.
- [3] Bateman, H. and Erdelyi, A. (1955). *Higher Transcendental functions*. Vol. 3, Mc Graw-Hill Book Company, Inc.
- [4] Beasley, J.E. and Christofides, N. (1989). *An Algorithm for the Resource Constrained Shortest Path Problem*. Networks 19, pp. 379 – 394.
- [5] Benkoski, S.J., Monticino, M.G. and Weisinger J.R. (1991). *A Survey of the Search Theory Literature*. Naval Research Logistics, Vol. 38, No. 4, pp. 468 – 494.
- [6] Chan, Y.K. and Foddy, M. (1985). *Real Time Optimal Flight Path Generation by Storage of Massive Data Bases*. Proceedings of the IEEE NEACON 1985, Institute of Electrical and Electronics Engineers, New York, pp. 516 – 521.
- [7] Dumitrescu, I. and Boland, N. (2001). *Algorithms for the Weight Constrained Shortest Path Problem*. ITOR, Vol. 8, pp. 15 – 29.
- [8] Dumitrescu, I. and Boland, N. (2001). *Improving Preprocessing, Labelling and Scaling Algorithms for the Weight Constrained Shortest Path Problem*. Submitted for publication to Networks.
- [9] Desrochers, M. and Soumis, F. (1988). *A Generalized Permanent Labeling Algorithm for the Shortest Path Problem with Time Windows*. INFOR 26, pp. 191 – 212.
- [10] Eagle, J.N. and Yee, J.R. (1990). *An Optimal Branch-and-Bound Procedure for the Constrained Path, Moving Target Search Problem*. Operations research, Vol. 38, No. 1, pp. 110 – 114.

- [11] Elsgohts, L.E. (1961). *Calculus of Variations*. Franklin Book Company, Inc.
- [12] Gelfand, I.M., Richard A. Silverman, Fomin, S.V. (2000). *Calculus of Variations*. Dover Publications, Inc.
- [13] Handler, G.Y. and Zang, I. (1980). *A Dual Algorithm for the Constrained Shortest Path Problem*. Networks 10, pp. 293 – 309.
- [14] Hassin, R. (1992). *Approximated Schemes for the Restricted Shortest Path Problem*. Mathematics of Operations Research 17, pp. 36 – 42.
- [15] Ince, E.L. and Sneddon, I.N. (1987). *The Solution of Ordinary Differential Equations*. Halsted Press.
- [16] Koopman, B.O. (1980). *Search and Screening: general principles with historical applications*. NY: Elmsford, Pergamon Press.
- [17] Mangel, M. (1984). *Search Theory*. Lecture Notes. Berlin: Springer-Verlag.
- [18] Skolnik, M.I. (1990). *Radar Handbook*, 2nd ed. New York: McGraw-Hill Book Company, Inc.
- [19] Stone, L.D. (1975). *Theory of Optimal Search*. New York, San Francisco, London: Academic Press.
- [20] Thomas, L.C. and Eagle, J.N. (1995). *Criteria and Approximate Methods for Path-Constrained Moving-Target Search Problems*. Naval Research Logistics, Vol. 42, pp. 27 – 38.
- [21] Vian, J.L. and More, J.R. (1989). *Trajectory Optimization with Risk Minimization for Military Aircraft*. AIAA, J. of Guidance, Control and Dynamics, Vol. 12, No. 3, pp. 311 – 317.
- [22] Washburn, A.R. (1983). *Search for a Moving Target: The FAB Algorithm*. Operations Research, Vol. 31, pp. 739 – 751.

Appendix

This appendix contains the derivation of the system of differential equations for determining an optimal risk path with a constraint on the path length and the analytical solution of this system for the case with a single radar.

We start with formulation of the calculus of variation problem with a nonholonomic constraint and a moveable end point

$$\min_{x, y} \Phi(x, y, \dot{x}, \dot{y}, l), \tag{1.A.1}$$

$$\Phi(x, y, \dot{x}, \dot{y}, l) = \int_0^l L(x(s), y(s), \dot{x}(s), \dot{y}(s)) ds, \quad (1.A.2)$$

$$\begin{aligned} x(0) &= x_1, & x(l) &= x_2, \\ y(0) &= y_1, & y(l) &= y_2, \end{aligned} \quad (1.A.3)$$

$$\varphi(\dot{x}(s), \dot{y}(s)) = 0, \quad (1.A.4)$$

$$l \leq l_*. \quad (1.A.5)$$

A necessary condition for the existence of a functional extremum requires the total variation of the functional to be equal to zero. Constraint (1.A.5) implies that this is the problem with the movable end point, $(x(l), y(l))$ (variation of the total curve length, l , is not equal to zero). It should be taken into account that variations δx and δy are dependent due to nonholonomic constraint (1.A.4). Usually, to separate differential expressions in the functional variation, the Lagrange multiplier method is used. However, compared to the traditional approach, here, the multiplier $\lambda(s)$ depends upon variable s , since two degrees of freedom, variables x and y , are used to formulate the problem. Applying the Lagrange multiplier method to problem (1.A.1)-(1.A.5), the total variation of functional (1.A.2) with constraints (1.A.4) and (1.A.5) is rearranged in the form

$$\begin{aligned} \delta\Phi &= \int_0^l \left([L'_x - \frac{d}{ds}L'_x - \frac{d}{ds}(\lambda(s)\varphi'_x)] \delta x + [L'_y - \frac{d}{ds}L'_y - \frac{d}{ds}(\lambda(s)\varphi'_y)] \delta y \right) ds \\ &+ \left(L - \dot{x}L'_x - \dot{y}L'_y - \lambda(s)[\dot{x}\varphi'_x + \dot{y}\varphi'_y] \right) \Big|_{s=l} \delta l \equiv 0. \end{aligned} \quad (1.A.6)$$

Assuming variation δx to be independent, and choosing $\lambda(s)$ to turn the expression

$$L'_y - \frac{d}{ds}L'_y - \frac{d}{ds}(\lambda(s)\varphi'_y)$$

at the variation δy to zero, equality (1.A.6) is reduced to the system of differential equations

$$\begin{aligned} L'_x - \frac{d}{ds}L'_x - \frac{d}{ds}(\lambda(s)\varphi'_x) &= 0, \\ L'_y - \frac{d}{ds}L'_y - \frac{d}{ds}(\lambda(s)\varphi'_y) &= 0. \end{aligned} \quad (1.A.7)$$

The equation defining the moveable end point, l , is given by

$$\left(L - \dot{x}L'_x - \dot{y}L'_y - \lambda(s)[\dot{x}\varphi'_x + \dot{y}\varphi'_y] \right) \Big|_{s=l} = 0. \quad (1.A.8)$$

It can be shown that equations of system (1.A.7) have the first integral. Summing the first equation multiplied by \dot{x} with the second one multiplied by \dot{y} , we have

$$\dot{x} \left(L'_x - \frac{d}{ds}L'_x - \frac{d}{ds}(\lambda(s)\varphi'_x) \right) + \dot{y} \left(L'_y - \frac{d}{ds}L'_y - \frac{d}{ds}(\lambda(s)\varphi'_y) \right) = 0.$$

The left-hand side of this equality is a total differential. After integration it turns to the expression

$$L - \dot{x}L'_x - \dot{y}L'_y - \lambda(s) (\dot{x}\varphi'_x + \dot{y}\varphi'_y) = \text{const.} \quad (1.A.9)$$

Lagrange multiplier, $\lambda(s)$, is derived from (1.A.9)

$$\lambda(s) = \frac{L + \lambda_L - \dot{x}L'_x - \dot{y}L'_y}{\dot{x}\varphi'_x + \dot{y}\varphi'_y}, \quad \lambda_L = -\text{const} \geq 0. \quad (1.A.10)$$

Substituting (1.A.10) into (1.A.7), we obtain the system of differential equations for determining $x(s)$ and $y(s)$. In the case when constraint $l \leq l_*$ is active, i. e. $l = l_*$, equation (1.A.8) is excluded from the system for determining an optimal solution, since the total curve length is fixed and, therefore, the variation of l equals zero by definition. If constraint $l \leq l_*$ is inactive, then from (1.A.8) and (1.A.9) we have $\lambda_L = 0$.

For the case of optimization problem (1)-(3), function L defines the risk index at the point (x, y) , and hence, it depends on variables x and y only,

$$L(x, y, \dot{x}, \dot{y}) \equiv L(x(s), y(s)) = \sum_{i=1}^N \frac{\sigma_i}{(x(s) - a_i)^2 + (y(s) - b_i)^2}. \quad (1.A.11)$$

Function φ represents reformulated nonholonomic constraint (6)

$$\varphi(\dot{x}(s), \dot{y}(s)) = (\dot{x}(s))^2 + (\dot{y}(s))^2 - 1 = 0. \quad (1.A.12)$$

Substituting value $\dot{x}\varphi'_x + \dot{y}\varphi'_y = 2$ into formula (1.A.10), Lagrange multiplier, $\lambda(s)$, is rewritten as

$$2\lambda(s) = L(x(s), y(s)) + \lambda_L. \quad (1.A.13)$$

Using (1.A.7), (1.A.8), (1.A.11) and (1.A.13), the original optimization problem (1)-(3) for defining the optimal trajectory $(x(s), y(s))$ is reduced to the system of differential equations

$$\begin{cases} L'_x - \frac{d}{ds}(\dot{x}L) = \lambda_L \ddot{x} \\ L'_y - \frac{d}{ds}(\dot{y}L) = \lambda_L \ddot{y} \end{cases} \quad (1.A.14)$$

with boundary conditions (1.A.3) and (1.A.5). Only two equations from (1.A.12), (1.A.14) are independent, since equation (1.A.12) is the first integral of system (1.A.14). A pair of independent equations is chosen from (1.A.12) and (1.A.14) to simplify the derivation of the solution. Certainly, the obtained solution must satisfy (1.A.12) and (1.A.14). Obtaining an analytical solution for system (1.A.14) in the case of an arbitrary number of radars is still an open issue. We present the analytical solution of system (1.A.14) in the case with a single radar. Without loss of generality, let us assume that the radar is located at the origin of the system of coordinates, i. e. $a_1 = 0$, $b_1 = 0$, and that the risk factor $\sigma = 1$. In such a case,

$$L(x, y) = d^{-2} = (x^2 + y^2)^{-1}. \quad (1.A.15)$$

To simplify further transformations, we use the polar system of coordinates. The polar radius ρ and polar angle Ψ are related to Cartesian coordinates x and y in the following way

$$\begin{aligned} x(s) &= \rho(s) \cos \Psi(s), \\ y(s) &= \rho(s) \sin \Psi(s), \end{aligned} \quad (1.A.16)$$

$$\begin{aligned} \dot{x} &= \dot{\rho} \cos \Psi - \rho \dot{\Psi} \sin \Psi, \\ \dot{y} &= \dot{\rho} \sin \Psi + \rho \dot{\Psi} \cos \Psi. \end{aligned} \quad (1.A.17)$$

Using (1.A.16), (1.A.17) and rearranged function L

$$L(\rho(s), \Psi(s)) = \rho^{-2},$$

system (1.A.14) and equation (1.A.12) are converted to equalities

$$\begin{aligned} 2\rho^{-3} \cos \Psi + \frac{d}{ds} \left((\dot{\rho} \cos \Psi - \rho \dot{\Psi} \sin \Psi)(\rho^{-2} + \lambda_L) \right) &= 0, \\ 2\rho^{-3} \sin \Psi + \frac{d}{ds} \left((\dot{\rho} \sin \Psi + \rho \dot{\Psi} \cos \Psi)(\rho^{-2} + \lambda_L) \right) &= 0, \end{aligned} \quad (1.A.18)$$

$$(\dot{\rho})^2 + \rho^2 (\dot{\Psi})^2 = 1. \quad (1.A.19)$$

Equations of system (1.A.18) have the first integral. Subtracting the second equation multiplied by $\cos \Psi$ from the first one multiplied by $\sin \Psi$, we obtain

$$\begin{aligned} \sin \Psi \frac{d}{ds} \left((\dot{\rho} \cos \Psi - \rho \dot{\Psi} \sin \Psi)(\rho^{-2} + \lambda_L) \right) \\ - \cos \Psi \frac{d}{ds} \left((\dot{\rho} \sin \Psi + \rho \dot{\Psi} \cos \Psi)(\rho^{-2} + \lambda_L) \right) &= 0. \end{aligned}$$

After algebraic transformations

$$\frac{\ddot{\Psi}}{\dot{\Psi}} + 2\frac{\dot{\rho}}{\rho} + \frac{\frac{d}{ds}(\rho^{-2} + \lambda_L)}{(\rho^{-2} + \lambda_L)} = 0.$$

Being a total differential, the left-hand side of the equation above is integrated and the right-hand side is converted to an unknown constant a . Using the equality obtained by integration, value $\dot{\Psi}$ is presented as the function of ρ

$$\dot{\Psi} = \frac{a}{1 + \lambda_L \rho^2}, \quad a > 0. \quad (1.A.20)$$

By substituting (1.A.20) into (1.A.18) and (1.A.19), we obtain the differential system for defining $\rho(s)$ and $\Psi(s)$

$$\begin{cases} (\dot{\rho})^2 + \rho^2 (\dot{\Psi})^2 = 1 \\ \dot{\Psi} = \frac{a}{1 + \lambda_L \rho^2} \end{cases} \quad a > 0. \quad (1.A.21)$$

To solve system (1.A.21), the relation between differentials ρ and Ψ is used, i. e. if $\rho = \rho(\Psi)$ then

$$\dot{\rho} = \frac{d\rho}{d\Psi} \dot{\Psi}. \quad (1.A.22)$$

Based on (1.A.21) and (1.A.22), function $\rho(\Psi)$ must satisfy the nonlinear ordinary differential equation

$$\left(\frac{d\rho}{d\Psi}\right)^2 = a^{-2} (1 + \lambda_L \rho^2)^2 - \rho^2. \quad (1.A.23)$$

The solution of (1.A.23) is reduced to the integral representation for $\Psi = \Psi(\rho)$, i. e.

$$\Psi = a \int \frac{d\rho}{\sqrt{(1 + \lambda_L \rho^2)^2 - a^2 \rho^2}} + C'. \quad (1.A.24)$$

Taking into account condition $a^2 > 2\lambda_L$, we make the following change of the variable in integral (1.A.24)

$$\rho = \alpha\tau, \quad \lambda_L^2 \rho^4 - (a^2 - 2\lambda_L) \rho^2 + 1 = (1 - \tau^2) (1 - \kappa^2 \tau^2),$$

where α and κ are new constants defined through a and λ_L as

$$\kappa = \frac{a^2 - 2\lambda_L - a\sqrt{a^2 - 4\lambda_L}}{2\lambda_L}, \quad \alpha = \sqrt{\frac{\kappa}{\lambda_L}}, \quad 0 \leq \kappa \leq 1, \quad \lambda_L \geq 0. \quad (1.A.25)$$

Function Ψ is expressed by the elliptic integral of the first kind

$$\Psi = a \int \frac{\alpha d\tau}{\sqrt{1 - \tau^2} \sqrt{1 - \kappa^2 \tau^2}} + C' = a \sqrt{\frac{\kappa}{\lambda_L}} F \left[\arcsin \sqrt{\frac{\lambda_L}{\kappa}} \rho, \kappa \right] + C''. \quad (1.A.26)$$

Inverting function (1.A.26) with respect to variable ρ , and using the expression for the elliptic sine (see, for instance, [3]),

$$\operatorname{sn}[u, \kappa] = \sin(am(u, \kappa)) = \sin \phi, \quad u = \int_0^\phi \frac{dt}{\sqrt{1 - \kappa^2 \sin^2 t}},$$

we obtain the solution for equation (1.A.23) in the form

$$\rho(\Psi) = \sqrt{\frac{\kappa}{\lambda_L}} \operatorname{sn} \left[\sqrt{\frac{\lambda_L}{a^2 \kappa}} \Psi + C, \kappa \right], \quad C = -\sqrt{\frac{\lambda_L}{a^2 \kappa}} C''. \quad (1.A.27)$$

To simplify relations between constants λ_L , a , and κ in (1.A.25), parameter λ_L is expressed by a and κ

$$\lambda_L = \frac{a^2 \kappa}{(1 + \kappa)^2}, \quad 0 \leq \kappa \leq 1. \quad (1.A.28)$$

Substituting the value of (1.A.28) into expression (1.A.27), the final representation for $\rho(\Psi)$ is

$$\rho(\Psi) = \frac{1+\kappa}{a} \operatorname{sn} \left[\frac{1}{1+\kappa} \Psi + C, \kappa \right]. \quad (1.A.29)$$

Based on (1.A.16) and (1.A.29), we have the analytical solution for the optimal trajectory (x, y)

$$\begin{aligned} x(\Psi) &= \frac{1+\kappa}{a} \operatorname{sn} \left[\frac{1}{1+\kappa} \Psi + C, \kappa \right] \cos \Psi, \\ y(\Psi) &= \frac{1+\kappa}{a} \operatorname{sn} \left[\frac{1}{1+\kappa} \Psi + C, \kappa \right] \sin \Psi, \end{aligned} \quad (1.A.30)$$

with boundary conditions

$$\begin{aligned} x^2 + y^2 &= \rho_1^2, & \Psi &= \Psi_1 = \arccos \frac{x_1}{\rho_1}, \\ x^2 + y^2 &= \rho_2^2, & \Psi &= \Psi_2 = \arccos \frac{x_2}{\rho_2}, \end{aligned} \quad (1.A.31)$$

where $\rho_1 = \sqrt{x_1^2 + y_1^2}$, $\rho_2 = \sqrt{x_2^2 + y_2^2}$ and $0 \leq \Psi \leq \pi$ by definition.

Using the arc length differential in the form $ds = a^{-1} (1 + \lambda_L \rho^2) d\Psi$, derived from (1.A.20), the total length and optimal risk for the trajectory $(x(s), y(s))$ are

$$l = a^{-1} \int_{\Psi_1}^{\Psi_2} (1 + \kappa \operatorname{sn}^2 \left[\frac{1}{1+\kappa} \Psi + C, \kappa \right]) d\Psi, \quad (1.A.32)$$

$$R = \frac{a}{(1+\kappa)^2} \int_{\Psi_1}^{\Psi_2} (\kappa + \operatorname{sn}^{-2} \left[\frac{1}{1+\kappa} \Psi + C, \kappa \right]) d\Psi. \quad (1.A.33)$$

Values for a , κ , and C should be determined in terms of l_* and boundary conditions (x_1, y_1) , (x_2, y_2) . In the case when the length constraint is relaxed, the optimal path has bounded length denoted by \bar{l} . If $\bar{l} \leq l_*$, then the length constraint, $l \leq l_*$, is inactive and l coincides with \bar{l} . To determine the value of \bar{l} , the optimal path without constraint on the length should be calculated. For the case when the length constraint is relaxed we have $\lambda_L = 0$. This implies $\kappa = 0$ and the elliptic sine becomes $\operatorname{sn}[u, 0] = \sin u$. Expression (1.A.29) is simplified

$$\rho(\Psi) = a^{-1} \sin(\Psi + C),$$

and the optimal solution is presented

$$\begin{aligned} x(\Psi) &= (2a)^{-1} (\sin C + \sin(2\Psi + C)), \\ y(\Psi) &= (2a)^{-1} (\cos C - \cos(2\Psi + C)). \end{aligned} \quad (1.A.34)$$

System (1.A.34) represents the circle in the parametric form. Excluding parameter Ψ from the system, we obtain the well-known representation for the circle

$$(x - (2a)^{-1} \sin C)^2 + (y - (2a)^{-1} \cos C)^2 = (2a)^{-2}. \quad (1.A.35)$$

Based on solution (1.A.35), unknown constants a and C are determined from the boundary conditions (x_1, y_1) and (x_2, y_2) . If ϑ is the angle between vectors (x_1, y_1) and (x_2, y_2)

$$\vartheta = \arccos \left(\frac{x_1 x_2 + y_1 y_2}{\sqrt{x_1^2 + y_1^2} \sqrt{x_2^2 + y_2^2}} \right), \quad (1.A.36)$$

then

$$a = \frac{\sin \vartheta}{\sqrt{(x_2 - x_1)^2 + (y_2 - y_1)^2}}, \quad (1.A.37)$$

and value \bar{l} for the unconstrained path length is determined by a and ϑ

$$\bar{l} = \vartheta/a. \quad (1.A.38)$$

Notice that a is always nonnegative, since formula (1.A.36) defines the value of ϑ in interval $0 \leq \vartheta \leq \pi$ and, therefore, $\sin \vartheta \geq 0$ for all ϑ .

Consequently, if $\bar{l} \leq l_*$ then the optimal solution is given by (1.A.35), (1.A.37), and in the case when $l_* \leq \bar{l}$, the optimal path is determined by system (1.A.30), where a , κ , and, C must satisfy equation (1.A.32) under condition $l = l_*$.